Multi-objective design optimization for crash safety of a vehicle with a viscoelastic body and wide tapered multi-cell energy absorber using DOE method

M. Pasandidehpour, M. Shariyat

Faculty of Mechanical Engineering, K.N. Toosi University of Technology, Tehran, Iran

shariyat@kntu.ac.ir

Abstract

Due to the extensive use of cars and progresses in the vehicular industries, it has become necessary to design vehicles with higher levels of safety standards. Development of the computer aided design and analysis techniques has enabled employing well-developed commercial finite-element-based crash simulation computer codes, in recent years. The present study is an attempt to optimize behavior of the structural components of a passenger car in a full-frontal crash through including three types of energy absorptions: (i) structural damping of the car body, (ii) viscoelastic characteristics of the constituent materials of the bumper, and (iii) a proposed wide tapered multi-cell energy absorber. The optimization technique relies on the design of experimental (DOE) method to enables finding the absolute extremum solution through the response surface method (RSM) in MINITAB software. First, the car is modeled in PATRAN and meshed in ANSA software. Then, the full-scale car model is analyzed in ABAQUS/CAE software. The optimization has been accomplished through a multi-objective function to simultaneously, maximize the observed energy and minimize the passenger's deceleration. Results are verified by the experimental results and effects of using non-equal importance coefficients for the absorbed energy and passenger's deceleration in the multi-objective function are also evaluated. Influence of the optimized parameters on the frontal crash behavior of the vehicle body structure and passenger's deceleration is investigated, too.

Keywords: Multi-objective optimization, Crash safety, Design of experiment, Energy absorption, Response surface method.

1. Introduction

Since the skin panels of the car body are chosen thinner to reduce the vehicle body weight and, consequently, reduce fuel consumption and increase the speed and acceleration in modern cars, investigation of the occupant safety in the frontal crashes has become a crucial issue more than before. Considering the complexity of the materials geometry as well as their non-linear deformation and behavior in the crashes may not be accomplished through using discrete dynamic models, adequately. Crashworthiness analysis of the passenger cars is generally conducted based on the theory of nonlinear finite element by means of special computer codes. Vehicle behavior determination techniques go through various stages before the model becomes ready for analysis [1]. The material properties and the elastic behavior of structures and all parameters required for proper analysis of the vehicle have been obtained from reverse engineering of the tests on vehicle parts. During the past two decades, explicit finite element codes used in design process have brought about a revolution in car manufacturing industry. Vehicle simulation is carried out at the most basic level of vehicle design process. Evaluation of vehicle safety in crashes by means of the data obtained from the experiments can be very costly and time-consuming. Therefore, the computational methods will be more affordable in this case. In this light, the newly-emerged software has enabled the engineers to conduct highly-reliable crash analyses. Of course, it has been proven that these codes are

only reliable for structures with ductile materials and plastic deformation [2]. Car design process may be viewed as an optimization problem in which both the vehicle weight and economic, as well as vehicle safety should be taken into consideration. Therefore, based on the developments in the computer technologies, automobile manufacturers and designers have chosen to use the finite element codes to simulate crashes. Using these codes, they can achieve acceptable results that are much more cost effective than the experimental testing. Another advantage of this method is the possibility of rapid modifications in the acceptable models along with performing experiments. This is a very important step in optimization. Other advantages of this method include possibility of rapid model changing and conduction of many tests within an acceptable period of time, that are of great importance in model optimization. Nowadays, increasing the computers power has paved the ground for increasing consistency of crash simulations with test results. Currently, most of the simulations in automotive research centers are conducted based on about eight hundred thousand elements [3].

Many studies have been conducted and different methods have been proposed for optimization of complex nonlinear problems such as car crashes. Response surface method is one of the common methods that has been expressed in terms of basic simple polynomial functions, for this purpose [4,5]. Fang et al [6] investigated effects of different basic functions on accuracy of the response functions and concluded that polynomial basic functions generally provide acceptable responses for energy absorption objective function while higher level functions can be used to improve the accuracy of objective functions in cases where maximum acceleration is desired in a full-scale car model. In general, response surface method can provide generally optimal results in situations where basic functions are appropriately chosen and the analytical range is large enough. Local improvement methods such as successive response surface [7,8], Two-Step RSM-enumeration algorithm [9] and D-Optimality standard [10] can be used to reduce the calculation costs in this method. Other techniques used in non-linear optimization problems such crashes were investigated by Jin et al [11]. They compared response surface methods, Kriging Method (KM), radial basis function and Multivariate Adaptive Regression Splines (MARS) in the 14 different problems and finally the radial basis function was considered the best choice in both large-scale and small-scale problems.

In the present study, attempts are made to introduce an overall algorithm to optimize vehicle behavior of a passenger car in frontal crashes. Three sources are adopted for the energy absorption and a multi-objective optimization includes both the energy absorption and occupant's acceleration at the seat is accomplished. The full-scale model of an automobile was analyzed in the ABAQUS/CAE crash simulation computer code, in order to simulate the vehicle crash. The response surface method was employed using the MINITAB 17 software to achieve the optimized design.

2. Theory basis of the problem

2.1. Description of the discretization and constitutive laws used in the crash analysis

The skin, underframe, and all the thin shell-type sections are discretized by means of a 4-noded quadrilateral element. It is known that results of the first-order triangular elements are not reliable in structural analyses. As Fig. 1 shows, in the finite element code, this element is mapped into a square element in the natural coordinates to enable using the most accurate numerical integration, i.e., the Gauss-Legendre procedure.

In the elasto-plastic analysis of the deformations that follow the crash, the effective plastic stress may be defined based on the deviatoric stress.

In Eqs. (1) to (3), t is time, D_{ij}^P is the plastic portion of the deformation rate tensor, σ_{kk} is the trace of the stress tensor and δ_{ij} denotes the Kronecker Delta. In the present research, Drucker-Prager kinematic hardening plasticity model that uses definitions of the effective stress and strain concepts, is employed.

The viscoelastic nature of the materials of the bumper are modeled by the Wiechert model shown in Fig. 2. This model consists of many Kelvin and Maxwell sub-elements. The relevant stress and stress relaxation module are defined in Eqs. (4) and (5):

$$s_{ij} = \sigma_{ij} - (1/3)\sigma_{kk}\delta_{ij}$$

$$\sigma = \sqrt{3/2\, s_{ij}\, s_{ij}}$$

and the effective plastic strain may be defined as

$$\varepsilon^{pl} = \int_0^t \sqrt{2/3 D_{ij}^P D_{ij}^P}\ dt$$

$$\sigma(t) = \varepsilon_0 (\sum_{i=0}^n k_i e^{-t/t_{ri}} + k_\infty)$$

$$E(t) = \sum_{i=0}^n k_i e^{-t/t_{ri}} + k_\infty$$

where k_∞ denotes the long term module, and t_{ri} stands for the relaxation time.
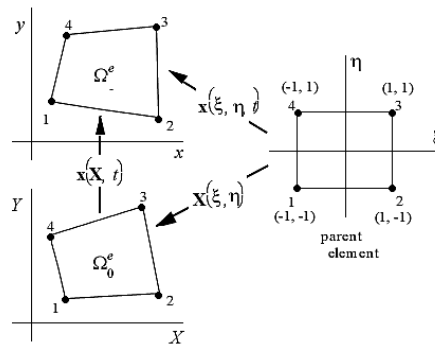

Fig1. Mapping the original quadrilateral element into the square element in the natural coordinates and vice versa, to carry out the computations and returning the results [12]
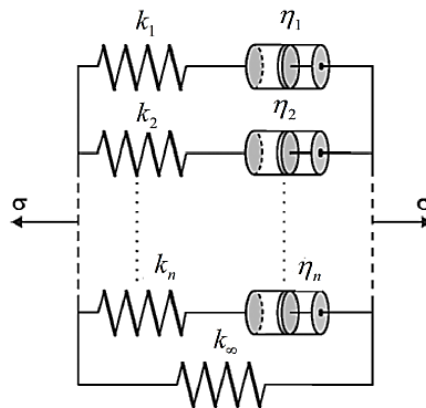

Fig2. Wichert viscoelastic model

Table 1 Factors and levels of the RSM

Factor	Variable	Level (1)	Level (0)	Level (-1)
A	Structural damping coefficient	0.04	0.02	0.0
B	Energy absorber thickness (mm)	2.0	1.5	1.0
C	Relaxation time of *polyurethane* material of the bumper (sec)	22.95	0.0023	0.0
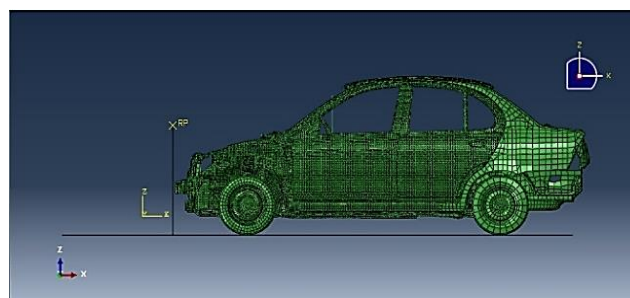
Fig3. . The full-scale finite element model of the considered passenger car

2.2. The employed model optimization algorithm

RSM is a set of useful mathematical and statistical methods for modeling and analyzing problems in which the demand function's response is affected by design parameter optimization is an attempt to achieve the desired value of response function. Appropriate response modeling for the independent input variables can be obtained, using regression analysis and design of experiments. In RSM the quantitative form a relationship between the desired response and independent input variables, as follows:

$$y = f(x_1 . x_2 . x_3 . \dots x_n) \pm \varepsilon$$

where y is the desired response, f is the response function (or surface response), $x_1 . x_2 . x_3 . \dots x_n$ are independent input variables, and ε shows the fitting error. Appropriate estimation of f determines the RSM success or failure. The data required to create response models is usually achieved through design of experiments. In the present research, the experimental data set of f is estimated using a second-order polynomial regression model. The second-order model of f may be defined as:

$$f = a_0 + \sum_{i=1}^{n} a_i x_i + \sum_{i=1}^{n} a_{ii} x_i^2 + \sum_{i<j}^{n} a_{ij} x_i x_j + \varepsilon$$

Where a_i represents the linear effect of x_i, a_{ii} shows the second order impact of x_i, and a_{ij} shows the linear-linear interaction between x_i and is x_j. Central composite design and Box-Behnken method are used to design and analyze problems. In the present study, the latter method is used to design experiments.

As no general rule is available for determining the samples in Box-Behnken method, the parameter limits are provided by the authors in the following tables. In the present study that includes three design variables, 2^2 full factorials are repeated three times. Table 1 shows the value of each factor and its coded value. The reasons for selection of each factor have been explained below.

3. Construction of the FE vehicle model and definition of the initial and boundary conditions

The full-scale model of the vehicle (a well-known passenger vehicle manufactures in Iran) with all its structural components have been used in this study. All components are modeled with shell elements and the components differ in thickness and type of material, the tire are modeled with membrane elements in such a way that equivalent vertical stiffness is provided for the tire. The engine model along with its real mass and moments of inertia is employed in the analysis. In this model the welded points are regarded as rigid connections (Fig. 3).

As mentioned in section 2,1n the shell elements used in this model are 4-noded rectangular elements. Materials used in the model are of viscoelastic and isotropic elasto-plastic types.

In this study, damage criteria are used to obtain results that are comparable to the experimental results. These criteria include ductile damage for the steel (ρ =7800 (kg/m^3), E=210 (GPa), σ_y =776 (MPa), σ_u =953 (MPa), ϑ =0.3) used in the car body, as well as shear ductile damage and FLD damage for more detailed modeling of wide tapered multi-cell energy absorber made of aluminum1060 (ρ =2700 (kg/m^3), E=68 (GPa), σ_y =113 (MPa), σ_u =147 (MPa), ϑ =0.3). This new design of energy absorber will be discussed in the optimization section.

Formability of sheets can be defined as their potential of deformation without rupture or necking. Sheets can be deformed only to a certain limit, and this limit is characterized by the beginning of local necking that ultimately leads to ruptures. Forming limit diagram (FLD) is one of the conventional techniques for determination of this limit. The diagram (Fig. 4) shows the ratio of major strain changes (ε_{major}) to the minor strain changes (ε_{minor}) at the necking moment.

The bumper was the first variable investigated in this section. Fig. 5 illustrates the bumper geometry. The viscoelastic (relaxation time) parameter of the constituent material of this component is regarded as an optimization factor.

This vehicle component that is the first part involved in the vehicle crash, plays an important role in vehicle energy absorption and reduction of acceleration of the occupant. Accordingly, influence of the viscoelastic nature of the materials of this component is investigated, I the present research. This type of modeling of viscoelastic bumpers in full-scale car model may be interesting and the results can be very valuable in various industries and provide the ground for extensive research on viscoelastic materials and their application in the automotive industry. The material properties of Polyurethane that is used in the vehicular industry are presented in Table 2. These properties are defined by calculation of their Prony series in the ABAQUS/CAE software. tri or the relaxation time that has a direct impact on the modulus of the material is used in order to compare the extreme states of Prony series. The non-viscoelastic property states were considered as optimization parameters.
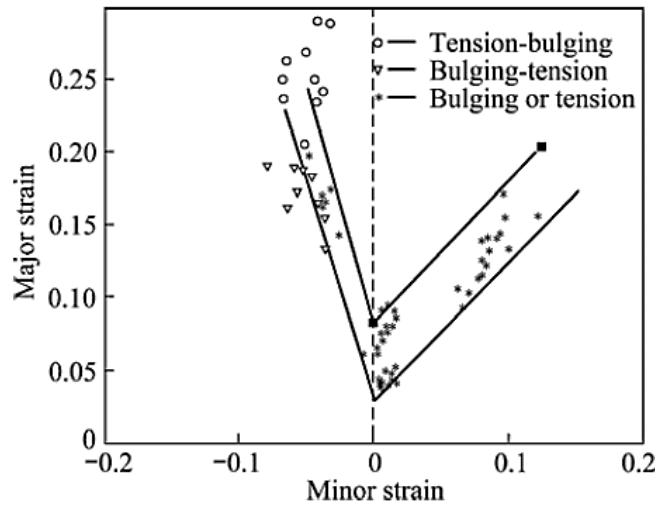
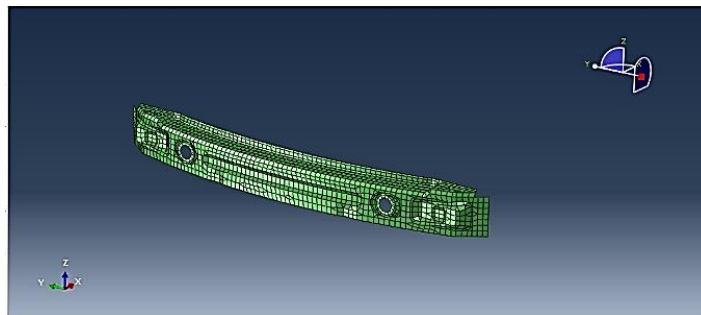**Fig4.** The forming limit diagram for the AL1060 alloy [13]

Fig5. The finite element model of the fascia bumper

Table 2 The considered viscoelastic parameters of the polyurethane [14]

i	1	2	3	4	5
tri (sec)	22.95	1.12	0.16	0.023	0.0023
Gi (Mpa)	1.85	4.04	15.0	43.28	107.45
G0 (Mpa)	1.115				
N	20				

The next optimization factor is energy absorbent that plays an important role in the energy absorption and reduction of acceleration force exerted on the occupants in frontal crashes. Therefore, the history of this component was investigated in the present study. According to the results obtained from previous studied on energy absorber [15] two factors known as specific energy absorption (SEA) and the crushing force efficiency (CFE) are two important factors in auto design processes and presented in the force-displacement graph in Fig. 6.
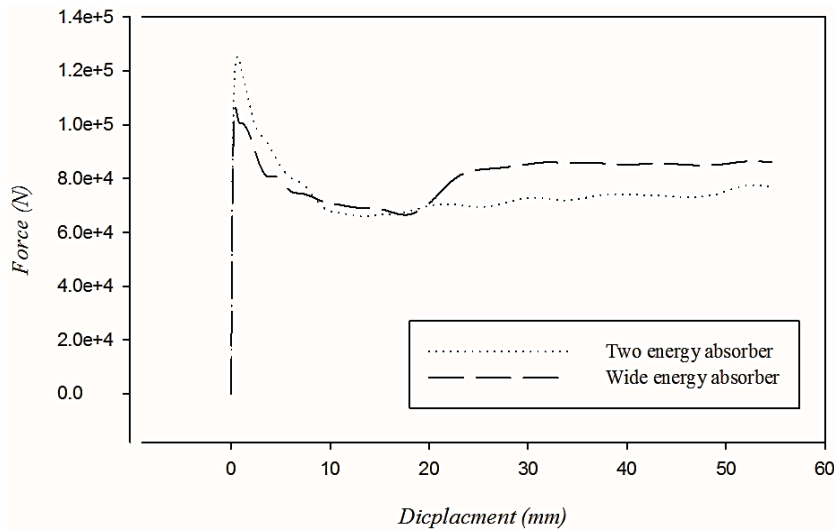
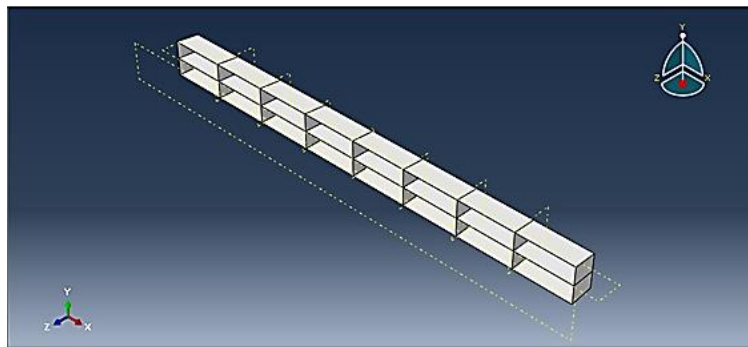**Fig6.** The energy absorber force-displacement graph corresponds to the present research

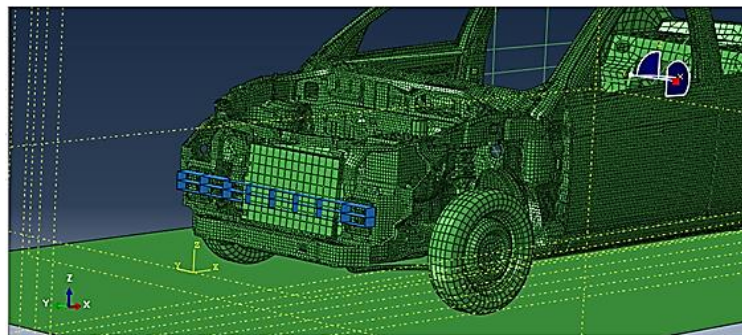**Fig7.** Design of the proposed wide tapered multi-cell energy absorber

Fig8. Location of installation of the wide tapered multi-cell energy absorber

Analysis of the proposed energy absorber in the ABAQUS/CAE and comparison of results with two other absorbers on the basis of SEA and CFE factors showed that a wide energy absorber behaves much better than bet two small assembled between two panels. In order to make sure about the accuracy of results, both absorber types made of the same material were tested on a full-scale car model and the results showed an improvement in the vehicle behavior in frontal crashes. Based on the results obtained from this test, we managed to present a completely new model to improve the energy absorbers behavior that

finally led to development of the energy absorber geometry shown in Fig. 7. This 1.125 * 0.05 (m) wide absorber is embedded behind the bumper. The constituent materials and the wideness of this absorber have enabled it to behave much better than two small absorbers on both sides of the vehicle. The location of this absorber on the car is presented in Figure 8.

The next factor taken into account in this section is the structural damping coefficient (viscose) of the vehicle body that significantly affects vehicle behavior in crashes. Considering the steel material used in the vehicle body, optimal values of this coefficient that are determined on the basis of Laboratory studies, range from 0 to 0.04.

4. Crash and Optimization analyses

4.1. Overview

In order to simulate the crash, the model analyzed in the ABAQUS/Explicit software in accordance with the Europe ECE R12 standard and was slammed into a rigid wall at 48 km / h.

As stated before, 3 parameters namely: viscoelastic nature of the bumper's material, damping coefficient of the vehicle body and the width of multicellular conical energy absorber were used to perform the ANOVA test based on design of experiments, and impact of these three parameters on the responses (the level of energy absorption and maximum acceleration of the occupant's body) was investigated.

4.2. The verification and initial experiments results

The car status after the impact and the results obtained from the analysis after simulation of the crash are shown in Fig. 9.

Verification of the FEM results of the base vehicle model has been accomplished through comparing the FEM results of the absorbed energy time history with that of the full-scale experimental ones reported by RICARDO Company, in Fig. 10. It was observed that error of present simulation is less than 2%. Time history of the acceleration of the occupant's body is shown in Fig. 10, for the base vehicle model.

As shown in Fig. 11, the graph of acceleration of the occupant has a maximum point or a peak that is used as one optimization objective function in this study and attempts are made to reduce value of this peak. In addition, in Fig. 10, which indicates the level of energy absorption during the crash, the peak which usually occurs at the end of the analysis period is considered as an optimization objective function to maximize its peak.

As mentioned in the previous section, some objective functions should be defined to optimize the model and considering the nature of this study, these functions aim to maximize the energy absorption while minimize the occupant's acceleration peak. Hence, this problem is considered to be a Multi-objective Optimization problem. To this end, the responses are extracted from each individual test and the impact of each parameter on them is investigated. The responses that are affected by these parameters are included in the final objective function. The test results according to objective functions that include absorbed energy by the vehicle and the acceleration of the occupants, for factors such as structural damping of vehicle body, bumper material and thickness of multicellular conical energy absorber are provided in the Table 4.
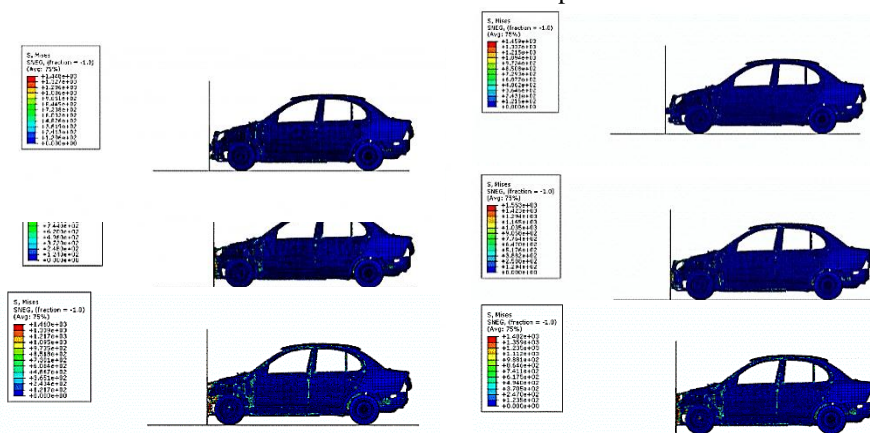

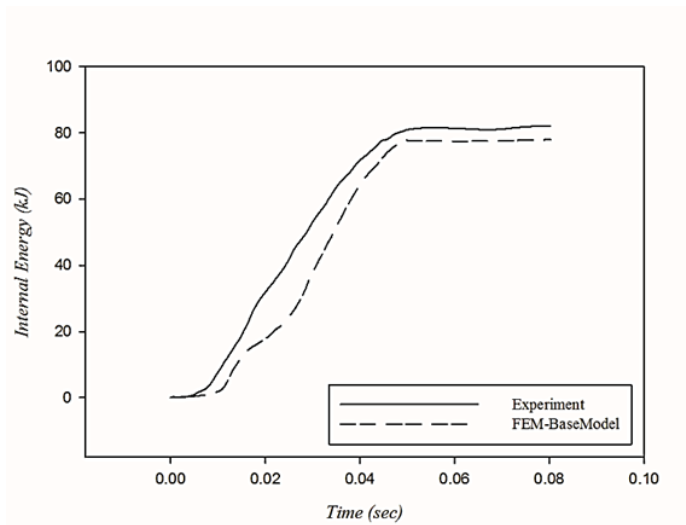**Fig9.** Vehicle status in time instants following the impact

Fig10. Verification of the present FEM results by the experimental results reported by RICARDO Company
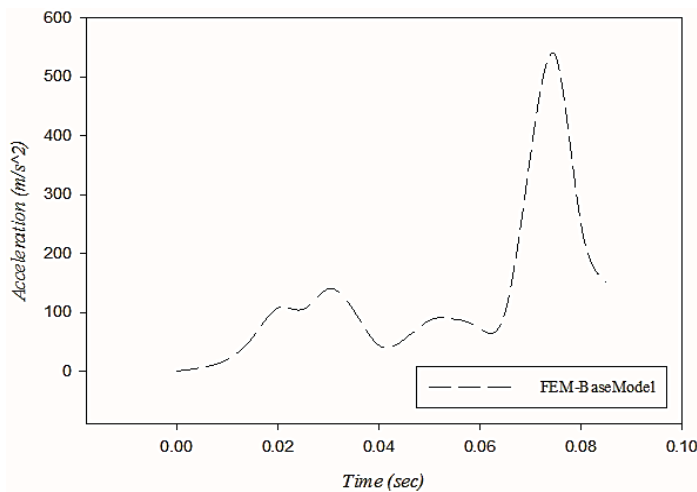

Fig11. Time history of acceleration of the occupant's body

4.3. Sensitivity analyses

The Results obtained from the 15 tests are entered into the MINITAB software as input data. This software performs the analysis of variance and obtains the regression equations for each response and finally provides some graphs and reports that can be used to decide whether each parameter has affected the responses.

Impact of different parameter combinations on the absorbed energy are reported in Table 5 and sample plots regarding effects of the parameters of the absorbed energy are shown in Figs. 12 and 13.

Analysis results and charts related to the acceleration of the occupant are provided in Table 5 and Figs. 14 and 15. According to Figs. 14 and 15, the minimum occupant's acceleration occurs when the B, C factors have been placed in the level 1 and A factor is set in the level 0.

As has been shown in the plots, the minimum occupant's acceleration occurs when the A, B factors have been placed in the level -1 and C factor is set to the level 0.

4.4. The optimization results

As the two-dimensional contour graph as well as the acceleration response and energy surface graphs

show, an optimal state is specified for each surface response.

So far, all the analyses and contours have been based on an objective function, but as mentioned before, we are looking for a case in which both objective functions are in the most favorable position. To find the area where the energy absorbed by the vehicle is at the maximum level and the acceleration of the occupants is at the minimum level at the same time, we consider some terms for the objective functions based on the obtained results, and keeping the bumper factor fixed (in state 1 that best fits both objective functions), we seek a response for the best area of structural damping coefficient and the thickness of multi-cell tapered energy absorber.

Table 4 the analysis results

Run order	A	B	C	Acceleration (m/s^2)	Energy (J)
1	-1	-1	0	538	88750
2	1	-1	0	581	89334
3	-1	1	0	592	91627
4	1	1	0	560	96512
5	-1	0	-1	641	85302
6	1	0	-1	452	90025
7	-1	0	1	353	93741
8	1	0	1	600	96113
9	0	-1	-1	598	95852
10	0	1	-1	643	91518
11	0	-1	1	535	97602
12	0	1	1	652	105758
13	0	0	0	624	97013
14	0	0	0	624	97013
15	0	0	0	624	97013

Table 5 The regression coefficients and impact of different parameter combinations on the absorbed energy

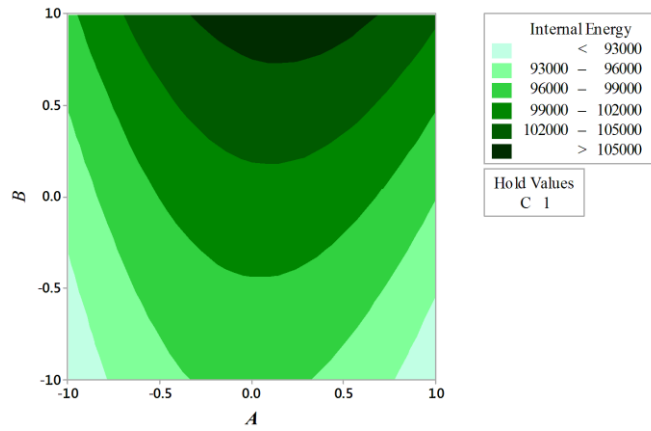| Term	Effect	Coefficient	T-Value	P-Value
Constant	-	97.01	38.94	0.0
A	3141	1571	4.27	0.008
B	3477	1738	4.72	0.005
C	7637	3818	10.37	0.0
A*A	11852	-5926	-10.94	0.0
B*B	938	469	0.87	0.426
C*C	416	208	0.38	0.716
A*B	2151	1075	2.07	0.094
A*C	1176	-588	-1.13	0.310
B*C	6260	3130	6.01	0.002

Fig12.   Contours of the absorbed energy in terms of factors A and B while fixing factor C is at level (1)
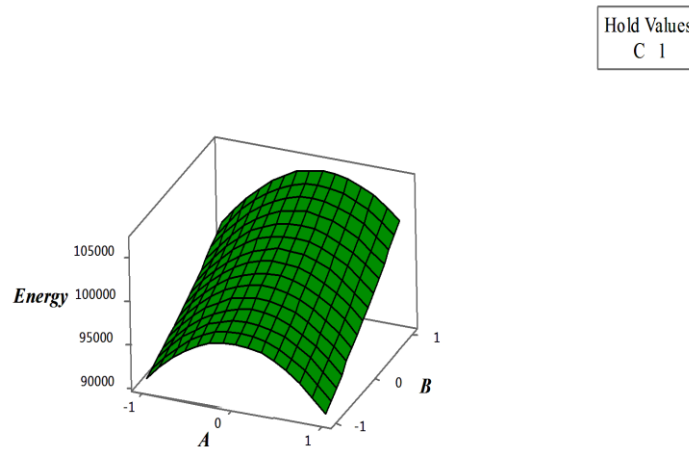

Fig13.   The surface plot of absorbed energy in terms of factors A and B, while the factor c is fixed at level (1)

Table 6 Regression coefficients and effects of different parameter combinations on the acceleration

Term	Effect	Coefficient	T-Value	P-Value
Constant	-	624	42.19	0.0
A	17.25	8.63	0.95	0.385
B	48.75	24.38	2.69	0.043
C	-48.5	-24.25	-2.68	0.044
A*A	-151.7	-75.9	-5.69	0.002
B*B	39.3	19.6	1.47	0.201
C*C	-73.2	-36.6	-2.75	0.04
A*B	-37.5	-18.8	-1.46	0.203
A*C	218	109	8.51	0.0
B*C	36.0	18.0	1.41	0.219
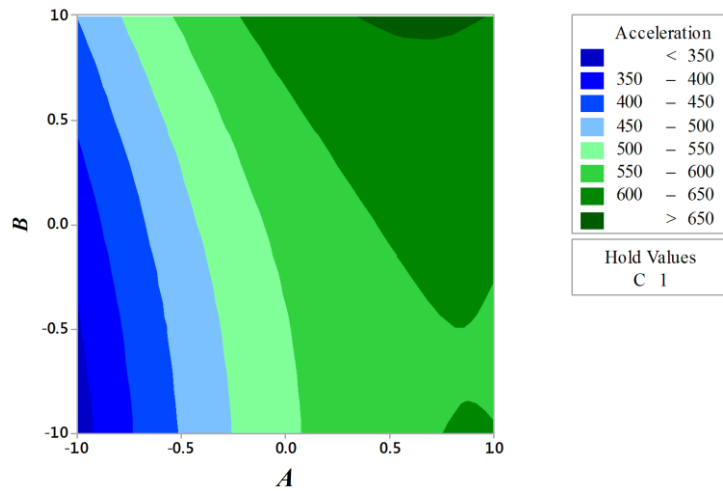
Fig14.   Contours of the occupant's acceleration in terms of factors A and B while factor c is fixed at level (1)
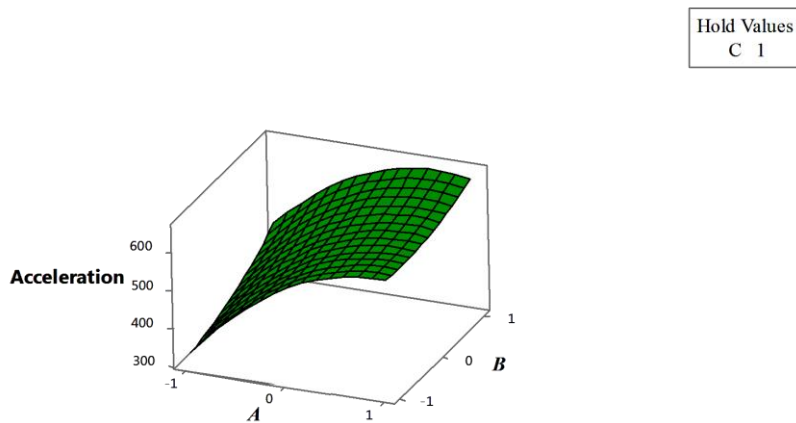
Fig15.   Surface plot of occupant acceleration in terms of factors A and B while factor C is at level (1)
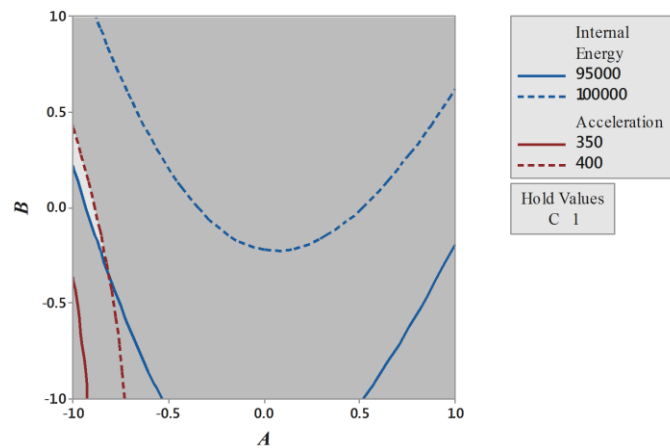

Fig16.   Contours of the feasible regions in terms of factors A and B, while fixing factor C is at level (1)

As shown in Fig. 16, the white area in our solution area that has satisfied all problem terms simultaneously and functions are placed in their optimal state. Terms applied in the multi-objective optimization process has shown in Table 7.

To have a better imagination of the absolute extremum responses presented in the next section, effects of each of the individual optimization factors on the responses is evaluated. Effects of the structural damping of the body material on the absorbed energy and occupant's acceleration are illustrated in Figs. 17 and 18, respectively. These figures reveal that considering the structural damping may enhance the energy absorption and occupant's acceleration reduction by 25 and 19 per cent, respectively. Effects of the tapered wide multi-cell energy absorber on the absorbed energy and occupant's acceleration are illustrated in Figs. 19 and 20, respectively. These figures reveal that considering the structural damping may enhance the energy absorption and occupant's acceleration reduction by 32 and 2 per cent, respectively. Therefore, while the improvement in the absorbed energy is remarkable, the reduction in the occupant's acceleration is minor.

Table 7 Terms applied in the optimization process

Objective	Target	Minimum limit	Favorable limit	Maximum limit	Weight	Importance
The total absorbed energy(kJ)	Maximum	85	105	105	1	1
Maximum longitudinal acceleration of the driver (m/s^2)	Minimum	353	353	652	1	1

Optimal values of level in each factor are shown in Table 8.

Table 8 Optimal values of the selected parameters

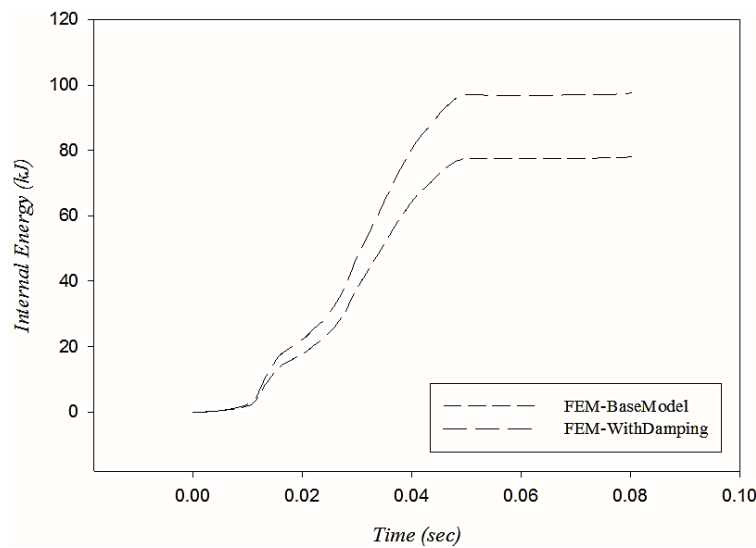| Viscoelastic bumper relaxation time (sec)	Energy absorber thickness (mm)	Structural damping coefficient
22.95	1.8182	0.0005

Fig17.   Time histories of the internal energy when considering/neglecting the structural damping of the body.
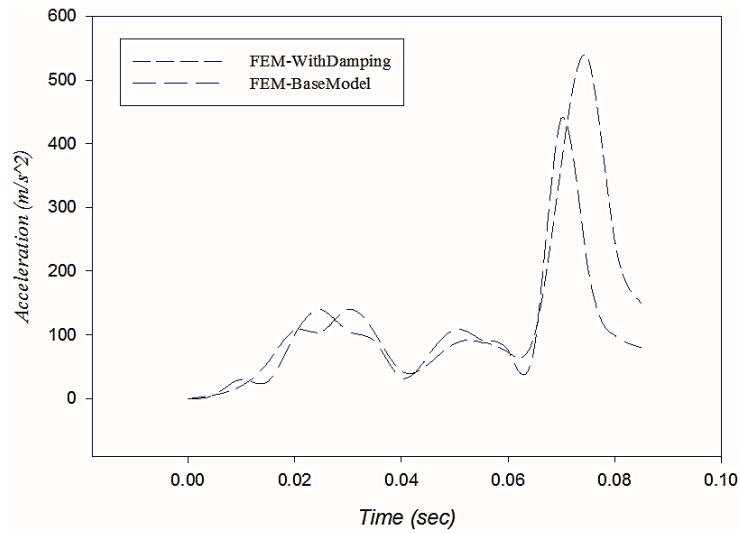
Fig18.   Effects of the structural damping on time history of the acceleration of the occupant's body
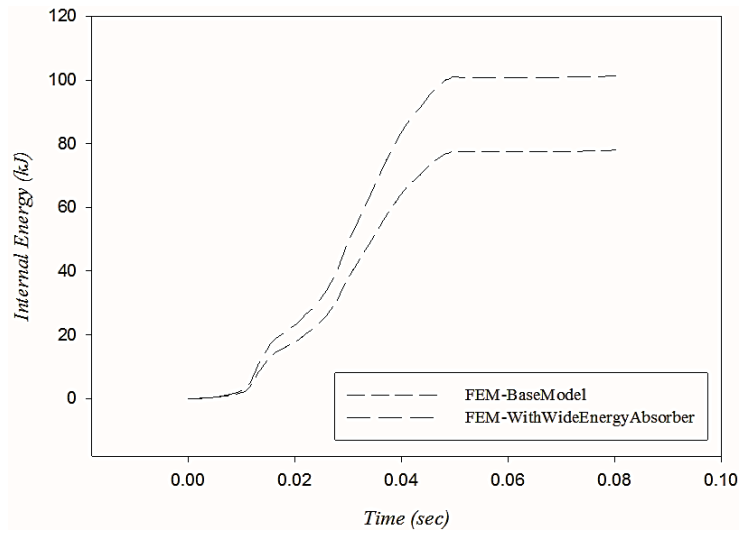
Fig19.   Time histories of the internal energy for designs with and without the tapered wide multi-cell energy absorber.
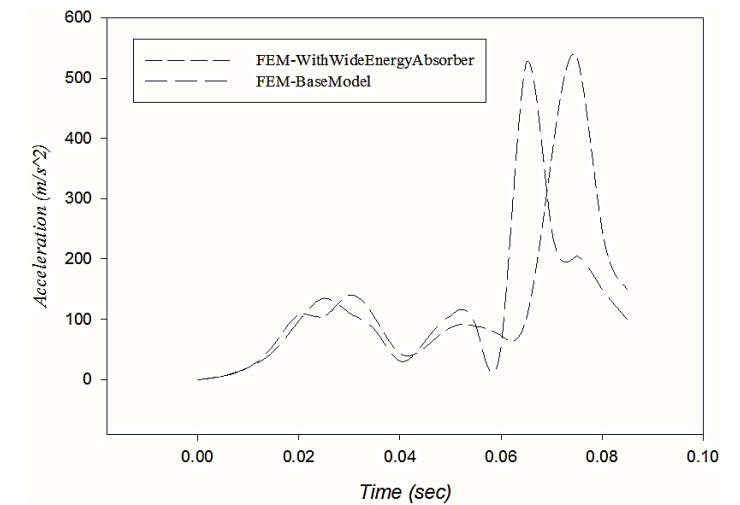
Fig20.   Effects of the proposed tapered wide multi-cell energy absorber on acceleration of the occupant's body.
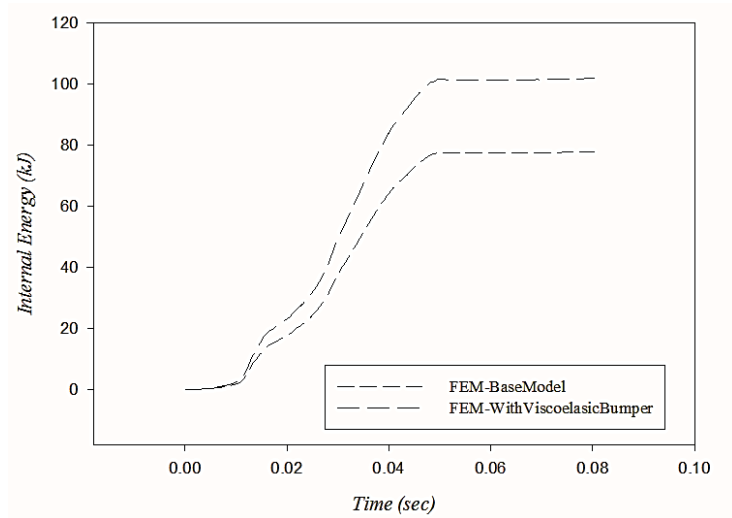
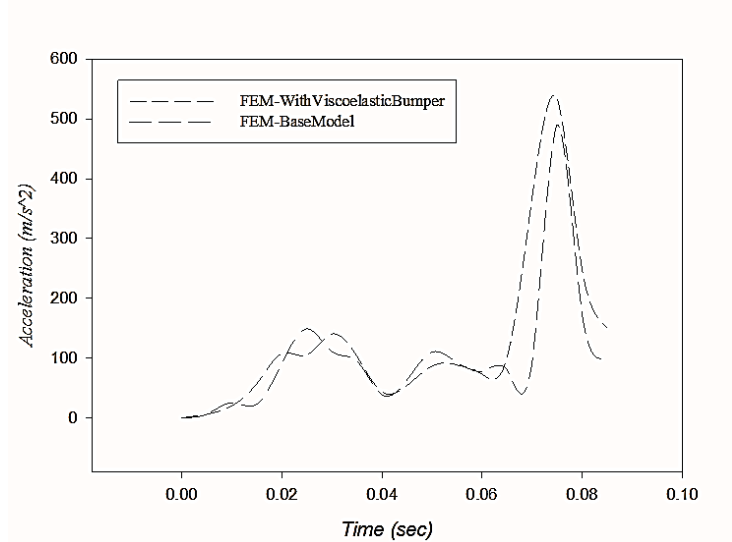**Fig21.**   Time histories of the internal energy for designs with elastic and viscoelastic bumpers

Fig22.   Figure 22 Effects of the viscoelastic nature of the bumper material on time history of the acceleration of the occupant's body

4.5. Results of the optimized model

After obtaining the optimum values for each parameter, the model was modified based on these values and reanalyzed afterwards. Comparison of the optimization results and base model results is provided in Table 9 as well as Fig. 23 and Fig. 24.

As the Figs. 23 and 24 show, improvement in the vehicle behavior in full-frontal crash is quite clear. The energy absorbed by the optimized model is much higher than the energy absorbed by the base model. Moreover, the optimized model shows hastened reductions in the peak of acceleration of the

occupant's body that is actually the goal of optimized model.

In the previous cases, weights of the absorbed energy and occupant's acceleration objectives were chosen identical. As a final stage results associated to cases where weights of the absorbed energy to occupant's acceleration is 5 to 1 and 1 to are reported in Figs. (25, 26) and (27,28), respectively

Table 9 Comparison of results of the optimization and original designs

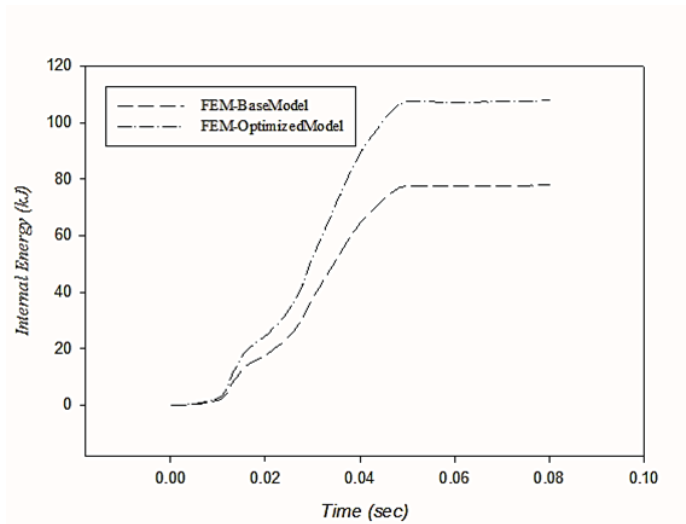| Objective	Base model	Optimized model	Improvement Percent
The total absorbed energy(kJ)	77.563	107.395	38.46 %
Maximum acceleration of the driver (m/s^2)	595.3292	395.872	33.50%

Fig23.   A comparison between time histories of absorbed energy, for the original and optimized designs
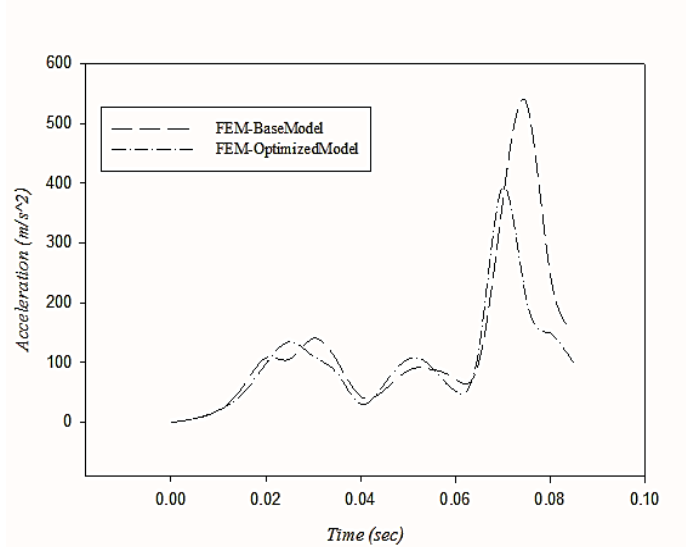

Fig24.   A comparison between time histories of accelerations of the occupant's body, for the original and optimized designs
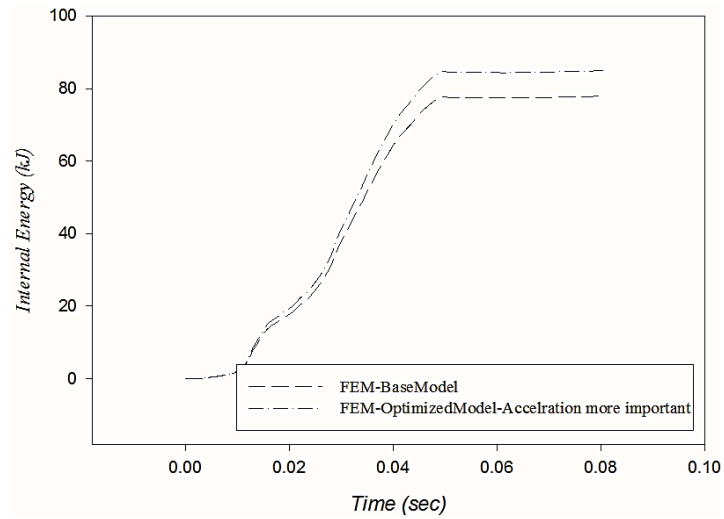
Fig25. A comparison between time histories of absorbed energy of the original design and optimized designs where the occupant's acceleration weight is 5 times that of the absorbed energy.
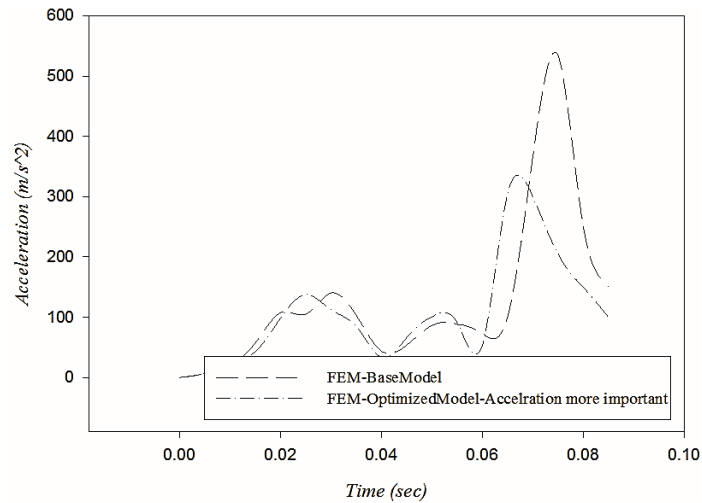

Fig26. A comparison between time histories of accelerations of the occupant's body, for the original design and optimized designs where the occupant's acceleration weight is 5 times that of the absorbed energy.
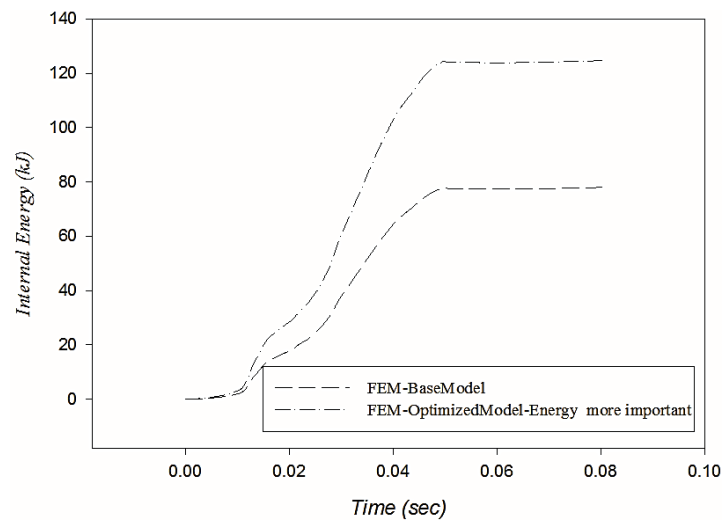

Fig27. A comparison between time histories of absorbed energy, for the original design and optimized designs where the absorbed energy weight is 5 times that of the occupant's acceleration
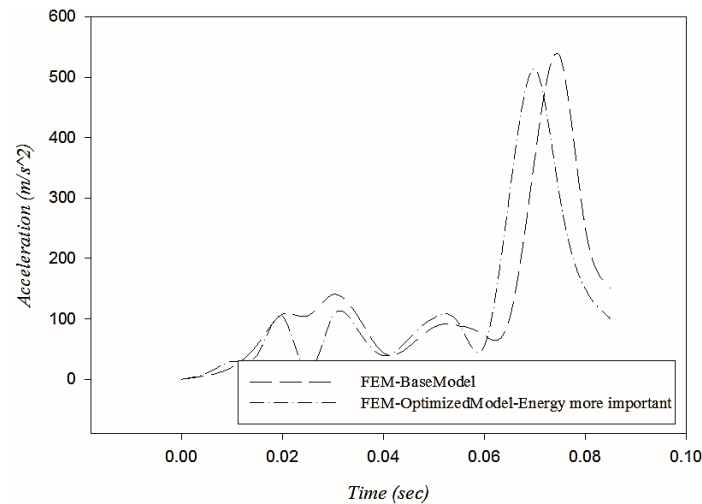
Fig28.   A comparison between time histories of accelerations of the occupant's body, for the original design and optimized designs where the absorbed energy weight is 5 times that of the occupant's acceleration.

5. Conclusions

The results presented in the results section, represent a relative improvement in energy absorption and maximum acceleration responses. This level of improvement is very suitable for energy absorption and application of the newly-introduced wide tapered multi-cell energy absorber has had a significant impact on energy absorption, which is about 38.4%. On the other hand, reduction in the maximum deceleration response directly shows significant reductions in the acceleration of the occupant (35.5%) and this indicates the efficiency of optimization factors in this study.

Results of this analysis indicate that addition of viscose damping properties can improve energy absorption behavior of the vehicle in full-frontal crashes and the use of viscoelastic materials in vehicle bumper can reduce the impact acceleration of the occupants, and lead to an increase in the energy absorption. Finally, the wide tapered multi-cell energy absorber, that serves as the most important factor in the present study, has significantly increased the energy absorption levels and reduced acceleration of the vehicle due to its geometry, thickness and constituent materials, and this fact has driven automotive manufacturers to use these initiatives to enhance vehicles safety.

References

[1]. .W. Kirkpatrick, Development and Validation of High Fidelity Vehicle Crash Simulation Models, SAE Technical Paper Series, 2000-01-0627

[2]. A.K. Pickett, T. Pyttel, F. Payen, F. Lauro, N. Petrinic, H. Werner, J. Christlein, Failure prediction for advanced crashworthiness of transportation vehicles, International Journal of Impact Engineering 2004;30:853-872

[3]. E. Joseph, R. M. Charles, Mechanical engineering design, 6th edition, McGraw Hill. 2001

[4]. H.B. Fang, K. Solanki, M.F. Horstemeyer, Numerical simulations of multiple vehicle crashes and multidisciplinary crashworthiness optimization, Int. J. Crashworthiness 2005;10 (2):161–171.

[5]. J. Forsberg, L. Nilsson, Evaluation of response surface methodologies used in crashworthiness optimization, Int. J. Impact Eng. 2006;32 (5): 759–777.

[6]. H. Fang, M. Rais-Rohani, Z. Liu , M.F.Horstemeyer, A comparative study of metamodeling methods for multiobjective crashworthiness optimization, Comput. & Struct. 2005;83(25–26): 2121–2136.

[7]. N. Stander, K.J. Craig, On the robustness of the successive response surface method for simulation based optimization, Eng. Comput. 2002;19 (4): 431–450.

[8]. H. Kurtaran, A. Eskandarian, D. Marzougui, Crashworthiness design optimization using successive response surface approximations, Comput. Mech. 2002;29 (4–5): 409–421.

[9]. Y.J. Xiang, Q. Wang, Z.J. Fan, H.B. Fang, Optimal crashworthiness design of a spot-welded thin walled hat section, Finite Elements Anal. Design 2006;42 (10):846–855.

[10]. M. Redhe, J. Forsberg, T. Jansson, P.O. Marklund, L. Nilsson, Using the response surface methodology and the D-optimality criterion in crashworthiness related problems, Struct. Multidisciplinary Optim. 2002;24 (3): 185-194.

[11]. R. Jin, W. Chen, T.W. Simpson, Comparative studies of metamodelling techniques under multiple modeling criteria. Struct Multidiscip Optim 2001; 23: 1-13.

[12]. J. Lemaitre, R. Desmorat, Engineering Damage MechanicsDuctile, Creep, Fatigue and Brittle Failures," Springer-Verlag Berlin Heidelberg 2005.

[13]. Comparative analysis between stress- and strain-based forming limit diagrams for aluminum alloy sheet 1060. Transactions of Nonferrous Metals Society of China. Trans. Nonferrous Met. Soc. China 2012;22:343−349

[14]. T. Sain, Rate dependent finite strain constitutive modeling of polyurethane and polyurethane–clay nanocomposites, International Journal of Solids and Structures 2015;54: 147–155.

[15]. A. Mahmoodi, M.H. Shojaeefard, H. Saeidi Googarchin. Theoretical development and numerical investigation on energy absorption behavior of tapered multi-cell tubes. Thin-Walled Structures102(2016)98–110